Available online at www.sciencedirect.com
SCIENCE DIRECT®
Synthetic Metals 155 (2005) 1–10
SYNTHETIC METALS
www.elsevier.com/locate/synmet

Poly(fluorene-oxadiazole) copolymer-based light-emitting devices on a plastic substrate

Shu-Jen Lee [a,b], Joseph R. Gallegos [c], Julien Klein [a], M. David Curtis [b,c], Jerzy Kanicki [a,b,*]

[a] *Organic and Molecular Electronics Laboratory, Department of Electrical Engineering and Computer Science, University of Michigan, Ann Arbor, MI 48109, USA*
[b] *Macromolecular Science and Engineering Center, University of Michigan, Ann Arbor, MI 48109, USA*
[c] *Department of Chemistry, University of Michigan, Ann Arbor, MI 48109, USA*

Received 21 June 2004; received in revised form 4 March 2005; accepted 6 May 2005
Available online 19 October 2005

Abstract

We reported on one new series of light-emitting copolymers for polymer light-emitting devices (PLEDs), poly(dioctyl fluorene-*co*-diphenyl oxadiazole)s (P(DOF-DPO)s). The device structure used in this study was composed of: indium tin oxide (ITO) anode/PEDOT:PSS ((polyethylenedioxythiophene)–poly(styrene sulfonate)) as hole-transporting layer/P(DOF) or P(DOF-DPO) as emissive layer/calcium + aluminum cathode. Both the photo-luminescence spectra and electro-luminescence spectra were slightly blue-shifted, when we added less than 10% DPO moiety into P(DOF-DPO). The maximum emission efficiency of the PLEDs based on P(DOF-DPO) with less than 10% DPO moiety are comparable to the P(DOF)-based PLEDs. However, when we added more than 20% DPO moiety into P(DOF-DPO), we found that P(DOF-DPO) PLEDs had significantly lower device efficiency than P(DOF) (poly(dioctyl fluorene)) PLEDs.

Keywords: Polymer light-emitting devices (PLEDs); Poly(dioctyl fluorene-*co*-diphenyl oxadiazole); Device efficiency

1. Introduction

Many researchers have accepted that the external quantum efficiency of organic polymer light-emitting devices (PLEDs) is limited by several major losses: charge injection at the contacts (anode and cathode), charge transport within the organic materials, electron and hole radiative recombination, photo-luminescent efficiency, and light out-coupling efficiency [1]. To achieve PLEDs with high efficiency and long lifetime, one basic requirement is needed: balanced electron and hole current, which results from balanced charge injection and transport.

Different approaches have been employed to balance the electron and hole current within a device. The first approach uses a multilayer device structure. The multilayer device structure effectively enhances device efficiency by incorporating an electron transport/injection layer (ETL/EIL) between an active emissive layer (EL) and a cathode [2] and/or a hole-transport/injection layer (HTL/HIL) between an EL and an anode [3]. However, for polymer-based devices, the multilayer device requires careful selection of materials and solvents to avoid damage of the polymer layers during the layer-by-layer, wet spin-coating process. Another drawback of the multilayer device is that it sometimes results in an unfavorable increase in device turn-on voltage [4]. The second approach uses a blend of emissive polymer with charge transport material as an active emissive layer [5,6]. The polymer blend device could possibly enhance device efficiency. However, some complications might occur; these include a variation in emissive color with varying current and phase separation during storage and operation [7]. The third approach lowers the hole injection barrier by a modification of the anode surfaces and electron injection barrier

* Corresponding author. Tel.: +1 734 936 0972; fax: +1 734 615 2843.
E-mail address: kanicki@eecs.umich.edu (J. Kanicki).

0379-6779/$ – see front matter © 2005 Elsevier B.V. All rights reserved.
doi:10.1016/j.synthmet.2005.05.018

by a use of low work function metals [8]. This approach could effectively enhance device efficiency by one or two orders of magnitude by matching the HOMO/LUMO (highest occupied molecular orbital/lowest unoccupied molecular orbital) level of emissive polymers with the anode/cathode work function, respectively. However, the electron and hole current might not be balanced due to a mismatch of electron and hole mobilities within emissive polymers. Therefore, some research has been dedicated to a molecular design of emissive polymers [7].

Several groups have been actively pursuing simplified fabrication processes for PLEDs by using emissive polymers with balanced charge injection and transport [7,12]. One widely studied series of emissive polymers is poly(phenylene vinylene)s (PPVs) [9,10]. To improve the electron transport property of PPV, researchers incorporated high electronegative moieties, such as oxadiazole [11] and cyano groups [3], into polymer main chains [12,13] or side chains [7,14]. Peng et al. [12] demonstrated that a PLED with an oxadiazole-containing PPV shows an external efficiency of 0.15%, 40 times higher than that of its corresponding PPV base polymer.

Another widely studied series of emissive polymer is poly(fluorene)s (PFO)s [9,10,15,16]. Poly(dioctyl fluorene) (P(DOF)) is known as a highly fluorescent blue-light-emitting material with an ionization potential of 5.8 eV and an electron affinity of 2.12 eV [17]. Also, P(DOF) exhibits strong non-dispersive hole-transport with high carrier mobilities, typically 10^{-3} $cm^2/(V\,s)$ at applied fields of 0.5 MV/cm, according to time-of-flight measurements [18]. However, P(DOF) exhibits a much weaker and highly dispersive electron transport with no clear transit time [18]. Therefore, to improve the electron transport property of P(DOF) or other conjugated polymers, high electronegative moieties, such as oxadiazole [11], phenylenecyanovinylene [3], quinoxaline, and quinoline [19], have been recently incorporated into polymer main chains [20–22] or side chains [23]. It is noted that the performance of single-layer P(DOF)-based PLEDs is limited by both the high injection barriers of holes and electrons and a mismatch of the electron and hole mobilities. It is also noted that an ohmic hole injection is possible from a PEDOT:PSS conducting polymer anode into P(DOF) by electrically conditioning the device at voltages higher than the electroluminescence turn-on voltage [24].

In our previous work, we reported device data based on a series of oxadiazole-containing fluorene copolymers [20]. Our rationale for synthesizing poly(dioctyl fluorene diphenyloxadiazole) P(DOF-DPO) is two-fold. The first potential advantage is that high device efficiency could possibly be achieved by covalently combining the emissive property of the P(DOF) and the electron transport property of the diphenyloxadiazole component without creating the microphase separation between two components. The second potential advantage allows us to adjust the emissive color by changing the proportions of the two components. In this paper, we report on the synthesis and characterization of this series of copolymers and on the performance of bi-layer PLEDs fabricated with P(DOF-DPO) and P(DOF) on plastic substrates [25]. In our study, we note that the hole injection barriers for P(DOF)-based device is high. Therefore, we employ a bi-layer device structure (PEDOT:PSS hole-transporting layer/P(DOF) or P(DOF-DPO) emissive layer) to minimize the hole injection barrier when we compare the device performance.

2. Experimental

2.1. Synthesis of the monomers

2.1.1. Synthesis of 2,5-(4-bromophenyl)-l,3,4-oxadiazole

2,5-(4-Bromophenyl)-l,3,4-oxadiazole was prepared with slight modifications to the report made by Lagrenée and coworker [26] (Scheme 1 in Fig. 1(a)). 4-Bromobenzoic acid (20.1 g, 0.1 mol) was placed in a three-necked flask fitted with a mechanical stirrer and a nitrogen inlet. The third neck was left open as a gas exhaust port. A nitrogen flow was kept over the flask for the entire course of the synthesis. In a separate flask, phosphorous pentoxide (42.6 g, 0.3 mol) was added slowly to 30 mL orthophosphoric acid with stirring, and the mixture was then allowed to cool to room temperature. Once cool, hydrazine dihydrochloride (5.25 g, 0.05 mol) was added and mixed thoroughly. This mixture was then added to the three-necked flask and stirred until a pasty mixture was achieved. Phosphorous oxychloride (15.3 g, 0.15 mol) was then added dropwise to the stirred mixture in the three-necked flask. The viscous mixture was slowly heated to 135 °C over a period of 2 h. After cooling to room temperature, 1.0 L of cool, deionized (DI) water was added with stirring, resulting in the precipitation of a white solid. The solid was then collected by filtration and washed with a (5%) $NaHCO_3$ solution followed by H_2O. The product was rinsed three times with methanol (200 mL) to remove an unidentified yellow byproduct. The washed white solid was collected, dried, and then recrystallized from 'the analysis' by ^1H NMR revealed a slight downfield shift for the aromatic protons as expected due to further deshielding. No aliphatic proton resonances were seen that would be symptomatic of incomplete ring closure. Further examination with FT-IR gave no evidence of carbonyl stretching. Elemental analysis reported expected product mass to within 0.5% by weight; mp: 269–271°. ^1H NMR ($CDC1_3$): δ 8.02 (4H, d), δ 7.70 (4H, d). MS for $C_{14}H_8N_2O^{79}Br_2$ calc. 377.904; found 377.96.

2.1.2. Synthesis of 2,7-dibromofluorene

A flask was charged with fluorene (16.6 g, 0.1 mol) and $CHCl_3$ (~200 mL) at room temperature (Scheme 2 in Fig. 1(a)). In a separate flask, bromine (16.0 g, 0.1 mol) was poured into $CHCl_3$ (~50 mL) and then added dropwise to the first flask. The yellow solution was washed with $NaHCO_3$ (saturated, 2 × 50 mL) and $NaHSO_3$ (saturated, 50 mL) and

Scheme 1.

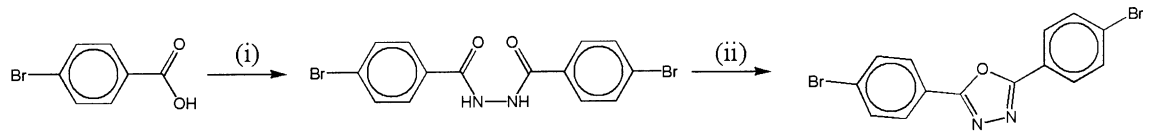

Scheme 2.

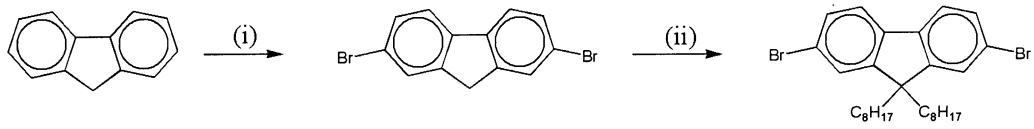

(a)

Poly(dioctyl fluorene-co-diphenyl oxadiazole), P(DOF-DPO)

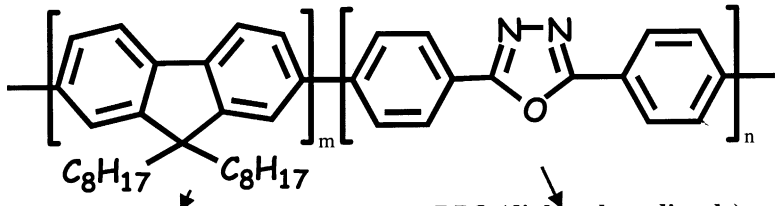

DOF (dioctyl fluorene)
highly fluorescent material

DPO (diphenyl oxadiazole)
good electron transport property

(b)

Fig. 1. (a) Synthesis schemes of the monomers—Scheme 1: (i) 4-bromobenzoic acid was added to a mixture of phosphoric acid, phosphorous pentoxide, and hydrazine dihydrochloride and stirred and (ii) phosphorous oxychloride added dropwise and the mixture is slowly heated. Scheme 2: (i) fluorene was cooled in $CHCl_3$, mixed with Br_2 and $FeCl_3$, then warmed to RT and (ii) *n*-octyl bromide was added and warmed to RT. (b) The chemical structure of the copolymers used in this work.

dried over $MgSO_4$. The solvent was removed and an off white product collected. Yield = 25.5 g (78.7%). ^{1}H NMR ($CDCl_3$): δ 3.87 (2H, s), δ 7.53 (2H, d), δ 7.61 (2H, d), δ 7.67 (2H, s).

2.1.3. Synthesis of 2,7-dibromo-9,9′-dioctylfluorene

A round bottom flask was charged with 2,7-dibromofluorene (4.3 g, 13.3 mmol), benzyltriethylammonium chloride (0.2 g, 0.9 mmol), 50% aqueous NaOH (5.0 mL), and DMSO (20 mL). The contents were stirred and kept under a nitrogen blanket. After a thorough mixture was achieved, 5.1 g (26.4 mmol) of octylbromide was added. The mixture was then stirred and heated to 80 °C for 1 h. The heat was removed, and the mixture stirred an additional hour. The reaction mixture was washed with toluene, then water, and dried over $MgSO_4$.The solvent was evaporated to yield a clear yellow viscous product. Analysis with the ^{1}H NMR revealed 70% dioctylfluorene with the remainder mono or non-reacted. The above octylation procedure was repeated on the sample until NMR analysis determined a 99% yield of dioctylfluorene solid. The product was purified by boiling in methanol and allowing to cool. The methanol was decanted and the procedure repeated until NMR analysis confirmed the removal of all traces of octylbromide. Yield = 5.2 g (72.0%). ^{1}H NMR ($CDCl_3$): δ 0.50–0.62 (4H, m), δ 0.78–0.91 (6H, t), δ 0.99–1.35 (20H, m), δ 1.82–1.95 (4H, m), δ 7.44 (2H, s), δ 7.46 (2H, d), δ 7.52 (2H, d).

2.2. Synthesis of the polymers

2.2.1. Synthesis of poly(dioctylfluorene-co-diphenyloxadiazole) (80:20)

Synthesis was carried out via a Ni^0-mediated aryl halide coupling, using $Ni(COD)_2$. This technique was used to polymerize similar monomers as reported by Curtis et al. [27]. A 250 mL round bottom Schlenk flask was charged with 2,5-(4-bromophenyl)-l,3,4-oxadiazole (0.11 g, 0.29 mmol), 9,9′-dioctylfluorene (0.64 g, 1.17 mmol) and a magnetic stir bar. The amounts were chosen to produce a 1:4 molar ratio, respectively, of the two monomers. The flask was evacuated and placed in a drybox. In the anaerobic environment, $Ni(COD)_2$ (0.70 g, 2.55 mmol) and 2,2′-bipyridine (0.40 g, 2.56 mmol) were added to the flask. The reaction vessel was then sealed and removed from the box. Dry, degassed toluene (∼100 mL) was added, and the system was allowed to reflux under a nitrogen blanket overnight. The reaction was monitored with a hand-held UV source (320–370 nm emission).

After 18 h of refluxing, the dark mixture was cooled and filtered through Celite. The Celite was rinsed with $CHCl_3$ until the filtrate was clear and colorless. The filtrate volume was reduced, and pouring the solution into stirred MeOH precipitated the product. The product was redissolved in toluene to free any encapsulated impurities and then precipitated in MeOH. The polymer was collected by filtration and dried under vacuum to yield a soft yellow polymer (Fig. 1(b)). Yield = 0.36 g (69.5%).

2.2.2. Synthesis of poly(dioctylfluorene-co-diphenyloxadiazole) (98:02) (90:10), and (60:40)

These syntheses followed the exact procedure described above for the 80:20 polymer, but with adjusted molar ratios of reactants. In all cases, the total moles of monomer used were 1.46 mmol. For the (98:02) copolymer, DOF (0.78 g, 1.43 mmol), and DPO (0.01 g, 0.03 mmol) are used. For the (90:10) copolymer; DOF (0.72 g, 1.31 mmol) and DPO (0.06 g, 0.15 mmol) are used. For the (60:40) copolymer, DOF (0.48 g, 0.88 mmol), and DPO (0.22 g, 0.58 mmol) are used.

2.3. Device fabrication

The P(DOF-DPO) PLEDs were fabricated on plastic substrates coated with pre-patterned indium tin oxide (ITO) [25]. Properties of this multilayer plastic substrate have been published in Ref. [25]. The ITO layer was used as a transparent anode in PLEDs with a sheet resistance of ∼10 Ω/□ and a transparency higher than 80% over the visible range (400–800 nm). The ITO-covered substrates were cleaned in an ultrasonic bath of isopropanol for 20 min and exposed to UV-ozone for 10 min before polymer spin-coating. In the first step of spin-coating, a hole-transport layer (HTL, 600 ± 100 Å) made from poly(3,4-ethylenedioxythiophene)–poly(styrene sulfonate) (PEDOT:PSS) was spin-coated from solution and thermally cured at 90 °C for 20 min. Then, an emissive layer (EL, 900 ± 100 Å) was spin-coated from a solution of P(DOF) or P(DOF-DPO) in xylene and cured at 90 °C for 1 h. Finally, a calcium cathode (∼150 Å) and then an aluminum cathode (∼2000 Å) as a capping layer were evaporated through shadow masks in a thermal evaporation system under a high vacuum (∼10^{-7} Torr).

2.4. Material and device characterizations

Characterization focused on opto-electronic properties of both the device and the materials. Absorption spectra, photo-luminescence (PL) spectra, and film thicknesses were measured with a CARY 5 UV–visible spectrophotometer, FluoroMax-2, and Dektak 3 surface profiler, respectively. The emissive layers used in these measurements were prepared on quartz substrates by spin-coating (∼1600 rpm, 10 s) with the same solution concentration (1.2%, w/v), resulting in a consistent film thickness of ∼1000 Å. The cyclic voltammetry (CV) data were measured with a CHI 660A model from the CH Instruments. The light-emitting polymer films were deposited on a platinum wire electrode in an electrolyte solution of $TBAPF_6$ (0.1 M) in CH_3CN. The potentials were measured relative to Ag/Ag^+ reference electrode (scan rate = 50 mV/s). Tapping mode atomic force microscopy images were carried out using a Digital Instruments NanoScope III Atomic Force Microscope. The photo-luminescence quantum efficiency measurements were performed using the integrating sphere method [28,29]. The electroluminescence (EL) was measured in the air by a CCD spectrum system with optical fibers, which has been calibrated with a tungsten filament lamp standard with known spectral irradiance (W/(cm^2 nm)), so the spectral flux (W/nm) of the PLEDs could be accurately measured. An integrated system consisting of an INS250 integrating sphere coated with barium sulfate from the international light, a programmable Keithley 617 electrometer, and a 230 voltage source was used for simultaneously collecting the optical and electrical data controlled by a home made program written in the Labview language [30,31]. The integrating sphere was calibrated to measure the total flux into the sphere system.

Therefore, the current–voltage–luminous flux (*I–V–L*) relationship was obtained. We then derived the luminance from the measured data by assuming a Lambertian angular distribution of the emission [32]. The power efficiency is defined as the total output of optical power (lumen) over the input electrical power (watt), and the emission efficiency is defined as the output light intensity (candela) over the input current density (ampere). The power and emission efficiencies could be derived from the *I–V–L* characteristics.

3. Results and discussion

3.1. Material properties

In this work, we hope to achieve higher PLED efficiency by a molecule design (covalently combining the emissive property of the poly(dioctyl fluorene) and the electron transport property of the diphenyloxadiazole (DPO) molecule). To achieve this, we had to optimize the ratio between the fluorescent and electron transport segments of the P(DOF-DPO) copolymers (see Fig. 1(b) for structure). To optimize the ratio between the two components, we synthesized four statistical copolymers with DOF:DPO feed molar ratios of 98:02, 90:10, 80:20, and 60:40. From our study, we obtained similar material and device properties for 98:02 and 90:10 P(DOF-DPO)s and also for 80:20 and 60:40 P(DOF-DPO); therefore, we focused our discussions on P(DOF), 90:10 P(DOF-DPO), and 80:20 P(DOF-DPO) in the following sections.

We determined and compared the material properties of P(DOF-DPO) with those of P(DOF) polymer, as listed in Table 1. Table 1 summarizes the properties of the polymers, including the molecular weight, ionization potential, electron affinity, and photo-luminescence quantum efficiencies.

Table 1
The molecular weight, ionization potential, electron affinity, and photo-luminescent quantum efficiency of the P(DOF-DPO) copolymers with different compositions, and the CIE coordinates of electro-luminescent spectra of the PLEDs

Sample	DOF (x)[a]	DPO (y)[a]	DPO composition[b]	Molecular weight (M_n)	I_p[c] (eV)	E_{a_1}[d] (eV)	E_{a_2}[e] (eV)	PL quantum efficiency[f] (%)	EL CIE[g]
P(DOF)	1	0	0	>100000	5.8	2.1	2.3	21 ± 5	0.234,0.264
90:10	0.9	0.1	0.10	>100000	5.8	2.1	2.3	17 ± 5	0.216, 0.225
80:20	0.8	0.2	0.16	>100000	5.7	2.1	2.3	13 ± 5	0.228, 0.249
DPO[h]	0	1	1	<10000	N/A	N/A	N/A	N/A	N/A

[a] x and y are feed molar ratios of DOF and DPO reactants, respectively. For details, see Section 2.
[b] The DPO composition was determined by CHN analysis.
[c] I_p is the ionization potential derived from the oxidation potential obtained by the cyclic voltammetry measurement.
[d] E_{a_1} is the electron affinity derived from the reduction potential obtained by the cyclic voltammetry measurement.
[e] E_{a_2} is the electron affinity obtained by a combination of the oxidation potential derived from the cyclic voltammetry measurement and the optical energy band gap derived from the UV–vis absorption spectroscopy.
[f] PL quantum efficiency is the measured photo-luminescent quantum efficiency of polymer films using an integrating sphere method.
[g] EL CIE is the CIE coordinate of the electro-luminescent spectra.
[h] When we tried to synthesize DPO polymer, DPO oligomer becomes insoluble and polymerization stops.

As can be seen in Table 1, the number average molecular weights of the polymers are above 100,000, suggesting that these polymers could have good film-forming properties by the spin-coating technique. The polydispersity index is ~1.7 for the light-emitting polymers used in this work.

The ionization potential (I_p) and electron affinity (E_{a_1}) are derived from the respective edges of the oxidation and reduction potentials obtained by cyclic voltammetry measurements (see Table 1; Fig. 2). In Fig. 2, we observe one oxidation peak and one reduction peak. Since it is believed that the edge of the oxidation potential ($E_{ox} \sim 1.46$ V versus $Ag/AgNO_3$ couple) represents the triggering point of the oxidation process [33], we used this value to define the highest occupied molecular orbital (HOMO) level of our emissive polymer. The edge of the reduction potential ($E_{red} \sim -2.3$ V versus $Ag/AgNO_3$) was used to calculate the lowest unoccupied molecular orbital (LUMO) level of the polymer. It is usually assumed that the ferrocene/ferrocenium (Fc/Fc+) oxidation potential ($E_{1/2} \sim 0.46$ V versus $Ag/AgNO_3$) corresponds to 4.8 eV versus the vacuum [33]. Hence, this factor may be used to estimate the I_p and E_{a_1} of the polymeric materials, thus defining the HOMO and LUMO levels, respectively (Table 1). Fig. 2 shows no significant changes on the ionization potential and electron affinity when DPO amounts were increased in the P(DOF-DPO) copolymers; therefore, the electron and hole injection barriers do not change significantly for our synthesized polymers.

We further calculated the optical band gap energy value ($E_G \sim 3.5$ eV) from the edge of the absorption peak in the absorption spectra (Fig. 3) [34], and extracted a different electron affinity (E_{a_2}) by using the HOMO level as the reference level. Since the optical band gap and HOMO level of the synthesized polymers did not change significantly with increasing DPO amount, no significant changes on the E_{a_2} were observed. It should be noted that values of I_p and E_a obtained by these methods represent a weighted average, so that no

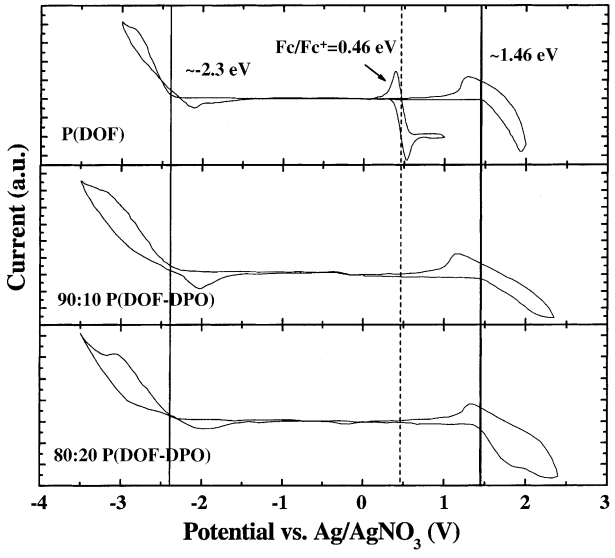

Fig. 2. The cyclic voltammograms of P(DOF), 90:10 P(DOF-DPO), and 80:20 P(DOF-DPO) light-emitting polymer films deposited on a platinum wire electrode in an electrolyte solution of $TBAPF_6$ (0.1 M) in CH_3CN. The potentials were measured relative to Ag/Ag^+ reference electrode (scan rate = 50 mV/s).

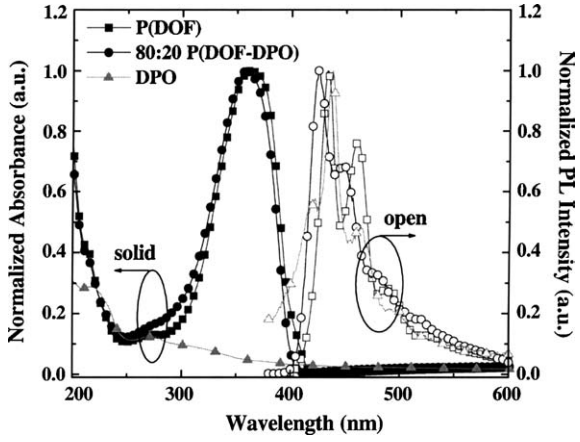

Fig. 3. The UV–visible absorption spectra and photo-luminescence spectra of P(DOF), 80:20 P(DOF-DPO), and DPO.

large changes are expected for relatively small amounts of DPO in the copolymer. However, on a microscopic level, the presence of DPO units might facilitate electron injection and transport.

Fig. 3 shows the normalized UV–visible absorption and photo-luminescence (PL) spectra of **P(DOF)**, **80:20 P(DOF-DPO)**, and **DPO**. Since all synthesized copolymers show similar UV–visible absorption and photo-luminescence spectra, we used **80:20 P(DOF-DPO)** data to represent the absorption and photo-luminance characteristics of copolymers. The PL spectrum of the P(DOF) polymer shows three main peaks at 434, 461, and 488 nm as shown in the literature [15,18], while that of **80:20 P(DOF-DPO)** shows three main peaks at 424,447, and 479 nm. The photo-luminescence spectrum of the **80:20 P(DOF-DPO)** copolymer is slightly blue-shifted in comparison with that of the P(DOF) polymer. Because DPO has a higher absorption in the shorter wavelength region, the UV–visible absorption spectrum of the **80:20 P(DOF-DPO)** copolymer is also slightly blue-shifted in comparison with that of the P(DOF) polymer.

The photo-luminescence quantum efficiencies of the P(DOF), **90:10** P(DOF-DPO), and **80:20** P(DOF-DPO) are 21 ± 5, 17 ± 5, and $13 \pm 5\%$, respectively. We observed a small decrease in the PL quantum efficiency when we added the DPO in the P(DOF-DPO) copolymers. The electron affinity of a molecule related to the P(DPO) molecule is estimated to be 2.5 eV, which is higher than that of P(DOF) (2.1 eV) [35]. Therefore, the DPO molecule might play role of the exciton or electron quenching centers for photo-luminescence. More specifically, the nitrogen and oxygen atoms on the DPO molecule have higher electronegativity in comparison with carbon; therefore, these nitrogen and oxygen atoms might play role of the quenching sites in copolymers.

We further investigated the surface topography of the polymer films by the atomic force microscopy (AFM) as shown in Fig. 4. The root-mean-square (RMS) roughness (R_q) of all synthesized emissive polymer films is 0.5 ± 0.2 nm over a 2 μm × 2 μm scan area, suggesting that the light emissive layer has a smooth surface. Also, no microphase segregation was observed for synthesized emissive polymer film in the phase AFM images. If the surface is not smooth enough or there is microphase segregation within the emissive layer, non-uniform field distribution inside the device can trigger localized degradation [25].

3.2. Opto-electronic characteristics of PLEDs

In our study, we note that the hole injection barriers for P(DOF)-based device is high. Therefore, we employ a bi-layer device structure (PEDOT:PSS (polyethylenedioxythiophene)–poly(styrene sulfonate)) as hole-transporting layer/P(DOF) or P(DOF-DPO) as emissive layer) to minimize the hole injection barrier when we compare the device performance.

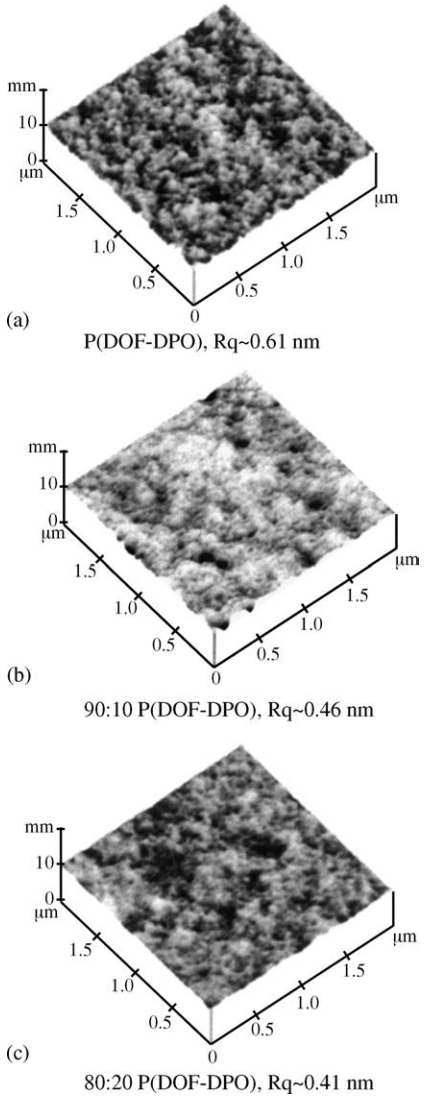

Fig. 4. The AFM images of: (a) P(DOF), $R_q \sim 0.61$ nm; (b) **90:10** P(DOF-DPO), $R_q \sim 0.46$ nm; (c) **80:20** P(DOF-DPO), $R_q \sim 0.41$ nm, light-emitting polymer films. The root-mean-square (RMS) average roughness (R_q) of the copolymer film surfaces is less than 1 nm over a 2 μm × 2 μm scan area.

The normalized electro-luminescence (EL) spectra of P(DOF) and P(DOF-DPO) PLEDs are plotted in Fig. 5. The EL spectrum of the P(DOF) polymer shows three main peaks at 435,451, and 483 nm, while those of copolymers show three main peaks at 426, 442, and 475 nm. The EL spectra of the copolymer with a DOF:DPO feed ratio of **90:10** are slightly blue-shifted and narrowed when compared with that of the P(DOF) polymer. This is because DPO has a higher absorption and photo-luminescence in the shorter wavelength region in comparison with DOF. The EL spectra of the synthesized polymers also show broadened emission spectra when compared with their PL spectra. The broadened EL spectra consist of three peaks of the PL spectra and one additional peak at 530 nm (this peak appears to be "bandtailing" phenomenon when its intensity is low). This EL broadening phenomenon has been investigated in the

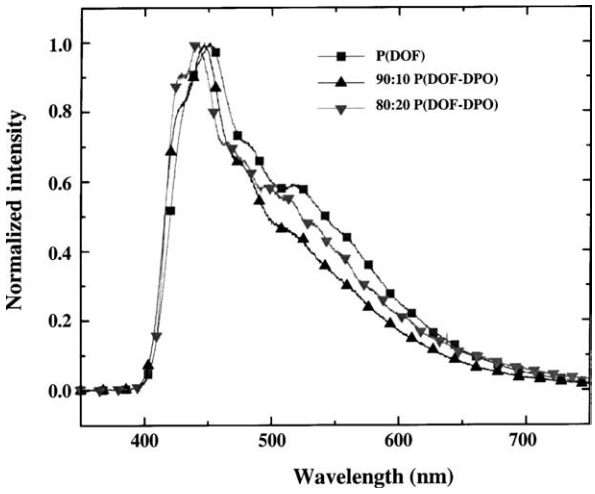

Fig. 5. The electro-luminescence spectra of P(DOF), **90:10** P(DOF-DPO), and **80:20** P(DOF-DPO) light-emitting polymers.

literature [36–38], and it is said to be induced by one of the following two possibilities. The first possibility is that there is a change of the polymer film morphology caused by thermal annealing of the polymer film during operation as a PLED. The effect of annealing results in partial crystallization, possibly assisted by the applied electric field. Excimer emission at a longer wavelength usually happens in the more ordered regions within crystalline domains, thus resulting in the bandtailing phenomenon seen in the EL spectra [36].

The second possibility is that there is a change of the polyfluorene segment at the 9,9-dialkyl site during the operation of the PLED. Because of this change, a part of 9,9-dialkyl fluorene has been observed to be oxidized as 9-fluorenone [37,38]. This defect formation can be induced either by photon emission or carrier injection and is accelerated by increase of temperature during light emission with the presence of oxygen. To confirm this oxidization process, List et al. have compared the PL spectra of poly(fluorene) and poly(*x*-fluorene-*co*-*y*-fluorenone) [37]. Even when the fluorenone concentration is as low as 5% in poly(*x*-fluorene-*co*-*y*-fluorenone), they have observed a strong additional PL emission peak at ∼530 nm associated with the defect light emission [37] in the PL spectrum of poly(*x*-fluorene-*co*-*y*-fluorenone), which poly(fluorene) does not show.

To investigate the EL broadening phenomena of our synthesized polymers, we annealed the 90:10 P(DOF-DPO) copolymer under vacuum and in air. As can be seen in Fig. 6(a), no significant change of the PL spectra was observed after we heated the 90:10 P(DOF-DPO) copolymer film at 90 °C for 1 h, then at 150 °C for an additional 1 h, and finally at 200 °C for 1 h under vacuum. We further investigated the change of the PL spectra after we heated the copolymer film at 200 °C for 1 h, immediately followed by shock cooling in liquid nitrogen [36]. We also did not observe a significant change of the PL spectra when the sample was heated and quenched in liquid nitrogen. Therefore, we concluded from our experiments that the EL broadening phenomena is less likely to be induced by the morphology change of the polymer film.

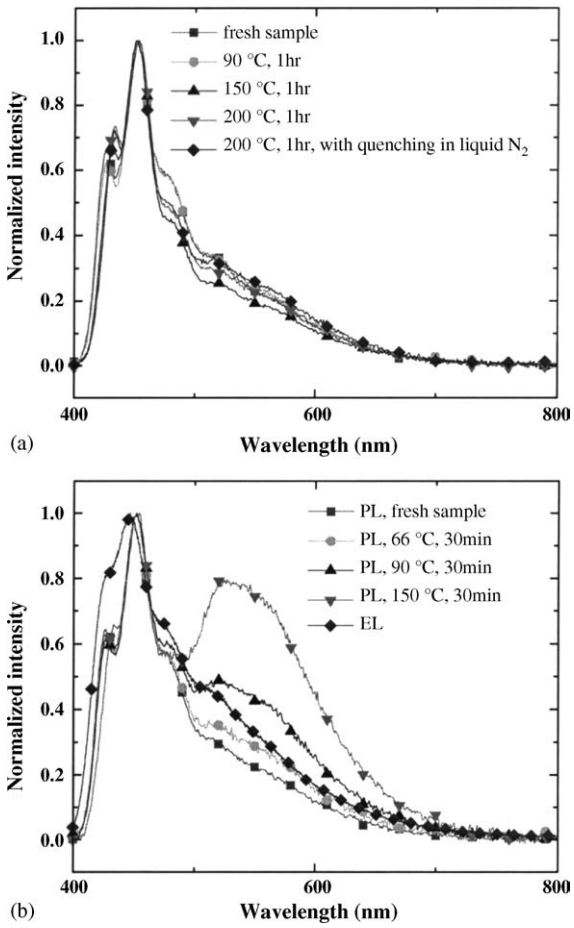

Fig. 6. The photo-luminescence spectra of 90:10 P(DOF-DPO) after heating: (a) under vacuum and (b) in air (the EL spectra of 90:10 P(DOF-DPO) is also included).

On the other hand, the broadening phenomena of PL spectra were clearly observed after we heated the 90:10 P(DOF-DPO) copolymer film at 66 °C for 30 min, then at 90 °C for 30 min, and then at 150 °C for 30 min in air (Fig. 6(b)). We also observed a new PL peak at ∼530 nm, as shown in the literature [37,38]. This peak was also observed in the EL spectrum; therefore, we concluded from our experiments that the EL broadening phenomena is associated with a change at the 9,9-dialkyl site of the fluorene segment. Since the intensity of this additional peak is small, the EL spectra appear to be a combination of main peaks of the PL spectrum and its bandtailing. After long-time operation (>1 h) of the PLEDs, the peak at 530 nm will increase its intensity and dominate the EL spectrum.

We further calculated the Comission Internationale de l'Éclairage (EL CIE) coordinates based on CIE 1931 chromaticity calculations [39]. These values are listed in Table 1. As can be seen in Table 1, the EL of P(DOF-DPO)

copolymers with less than 10% DPO show more saturated blue color when compared with P(DOF) polymer. When the amount of DPO is above 20%, the EL spectra of the P(DOF-DPO) are broadened slightly, thus shifting the CIE coordinate toward the center of the chromaticity diagram.

The characteristics of current density (J) versus voltage (V), luminance (L) versus voltage (V), and luminance (L) versus current density (J) are shown in Fig. 7(a–c), respectively, for bi-layer copolymer PLEDs fabricated on a plastic substrate. The device structure used in this study was composed of: indium tin oxide (ITO) anode/PEDOT:PSS hole-transporting layer (600 ± 100 Å)/P(DOF) or P(DOF-DPO) emissive layer (900 ± 100 Å)/calcium + aluminum cathode. Turn-on voltages defined at 1 cd/m^2 luminance level are 3.8, 4.6, and 5.2 V (Fig. 7(b)) and turn-on current densities defined at 1 cd/m^2 luminance level are 4.6, 9.6, and 35 mA/cm^2 (Fig. 7(c)) for P(DOF), **90:10** P(DOF-DPO), and **80:20** P(DOF-DPO), respectively. As can be seen in Fig. 7, the turn-on voltage and the turn-on current density of P(DOF-DPO)-based PLEDs are higher than that of P(DOF)-based PLEDs. We observed similar trends of turn-on voltage when we used aluminum as a cathode. The exact nature of the shift in turn-on voltage is not clear at the present time. As also can be seen in Fig. 7(c), when the current density is above 100 mA/cm^2, we observed that 90:10 P(DOF-DPO) PLEDs shows comparable luminance at same current density level in comparison with P(DOF) PLEDs. However, when we added DPO amount above 20%, we observed a strong decrease in the luminance at same current density level. Since DPO molecule has a relatively high electron affinity in comparison with DOF, the DPO molecule might play role of the exciton or electron quenching centers for electroluminescence.

Fig. 8 shows the characteristics of emission efficiency and power efficiency versus luminance. The emission efficiency is defined as the output light intensity (candela) over the input current density (ampere); and the power efficiency is defined as the total output optical power (lumen) over the input electrical power (watt). As can be seen in Fig. 8, the P(DOF-DPO)-based PLEDs with less than 10% DPO amount show comparable emission efficiency and less power efficiency when compared with the P(DOF)-based PLEDs. However, when we added more than 20% DPO into P(DOF), the efficiencies of P(DOF-DPO)-based PLEDs are significantly lower than those of P(DOF)-based PLEDs. Our experiments indicate two interesting things: (1) for PPV-based molecules, Peng et al. [12] and Bao et al. [14] have reported that higher device efficiency could be achieved by covalently combining the fluorescent property (PPV) and diphenyl oxadiazole (DPO) for a single-layer device. However, our experiments clearly indicate that this similar methodology does not apply for P(DOF-DPO). It is probably because DPO molecule has a relatively high electron affinity in comparison with DOF, the DPO molecule might play role of the exciton or electron quenching centers for electroluminescence. (2) We find that when we added a small amount (<10%) of DPO component

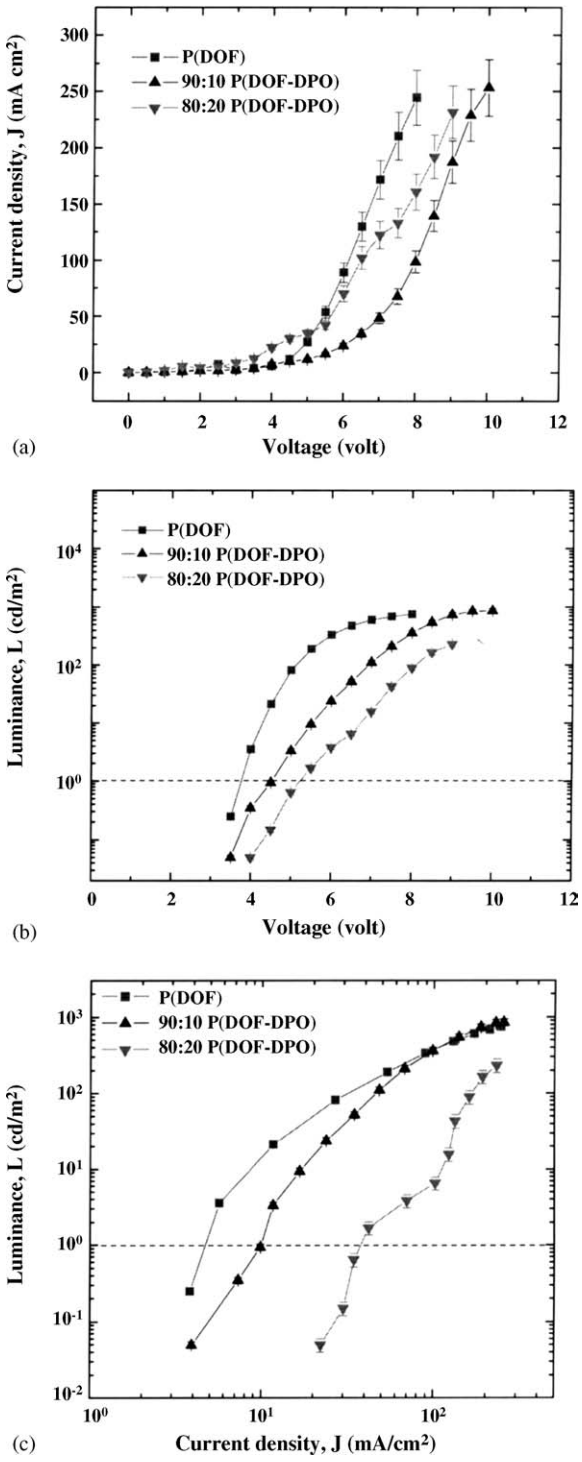

Fig. 7. (a) The characteristics of current density (J) vs. voltage (V). (b) The characteristics of luminance (L) vs. voltage (V), and the characteristics of luminance (L) vs. current density (J) for bi-layer PLEDs based on P(DOF), **90:10** P(DOF-DPO), and 80:20 P(DOF-DPO) light-emitting polymers. The PLEDs structure is ITO anode/PEDOT:PSS layer (∼60 nm)/light-emitting polymer layer (∼90 nm)/Ca (15 nm)/Al (200 nm) cathode.

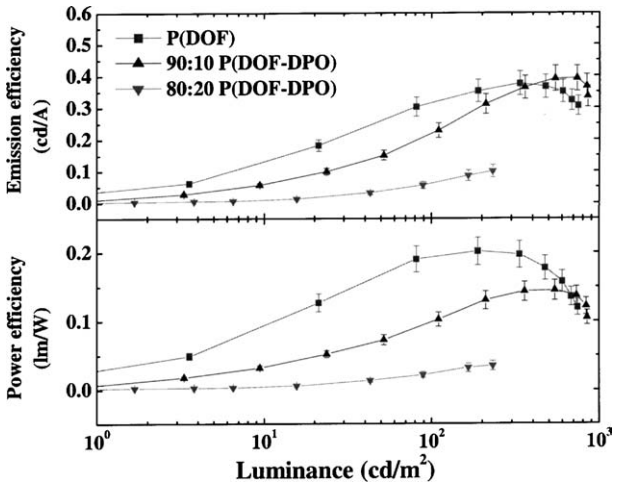

Fig. 8. The characteristics of emission efficiency and power efficiency vs. luminance for PLEDs based on P(DOF), **90:10** P(DOF-DPO), and **80:20** P(DOF-DPO) light-emitting polymers.

into P(DOF-DPO) copolymers, we obtain PLEDs with more saturated blue color.

4. Conclusions

We have synthesized and characterized one new series of light-emitting polymers based on poly(dioctyl fluorene-*co*-diphenyl oxadiazole)s, P(DOF-DPO). The AFM data suggested that the emissive layer has a smooth surface with RMS roughness about 0.5 ± 0.2 nm over a $2\,\mu m \times 2\,\mu m$ area. We have also studied the opto-electronic properties of PLEDs based on P(DOF-DPO) copolymers with different compositions. The maximum emission efficiency of the P(DOF-DPO)-based PLEDs is comparable to the P(DOF)-based PLEDs when we added less than 10% DPO. However, when we added more than 20% DPO moiety into P(DOF-DPO), we found that P(DOF-DPO) PLEDs had significantly lower device efficiency than P(DOF) (poly(dioctyl fluorene)) PLEDs. For PPV-based molecules, Peng et al. [12] and Bao et al. [14] have reported that higher device efficiency could be achieved by covalently combining the fluorescent property (PPV) and diphenyl oxadiazole (DPO) for a single-layer device. However, our experiments clearly indicate that this methodology does not apply for P(DOF-DPO)-based PLEDs. It is probably because DPO molecule has a relatively high electron affinity in comparison with DOF, the DPO molecule might play role of the exciton or electron quenching centers for electro-luminescence.

Acknowledgements

We thank National Institute of Health and National Science Foundation (NSF Grant No. DMR 9986123) for financial support. J.G. is thankful for support from IGERT (NSF Grant No. DGE 9972776).

References

[1] N.K. Patel, S. Cinà, J.H. Burroughes, IEEE J. Sel. Top. Quantum Electron. 8 (2002) 346.
[2] C. Adachi, T. Tsutsui, S. Saito, Appl. Phys. Lett. 55 (1989) 1489.
[3] N.C. Greenham, S.C. Moratti, D.D.C. Bradley, R.H. Friend, A.B. Holmes, Nature 365 (1993) 628.
[4] C. Adachi, T. Tsutsui, S. Saito, Appl. Phys. Lett. 56 (1990) 799.
[5] M. Uchida, Y. Ohmori, T. Noguchi, T. Ohnishi, K. Yoshino, Jpn. J. Appl. Phys. 32 (1993) L921.
[6] M. Strukelj, T.M. Miller, F. Papadimitrakopoulos, S. Sehwan, J. Am. Chem. Soc. 117 (1995) 11976.
[7] Y.Z. Lee, X. Chen, S.A. Chen, P.K. Wei, W.S. Fann, J. Am. Chem. Soc. 123 (2001) 2296.
[8] R.H. Friend, R.W. Gymer, A.B. Holmes, J.H. Burroughes, R.N. Marks, C. Taliani, D.D.C. Bradley, D.A. Dos Santos, J.L. Brédas, M. Loè Gdlund, W.R. Salaneck, Nature 397 (1999) 121.
[9] J.H. Burroughes, D.D.C. Bradley, A.R. Brown, R.N. Marks, K. MacKay, R.H. Friend, P.L. Burns, A.B. Holmes, Nature 347 (1990) 539.
[10] A. Kraft, A.C. Grimsdale, A.B. Holmes, Angew. Chem. Int. Ed. 37 (1998) 402.
[11] C. Zhang, S. Hoger, K. Pakbaz, F. Wudl, A.J. Heeger, J. Electron. Mater. 23 (1994) 453.
[12] Z. Peng, Z. Bao, M.E. Galvin, Chem. Mater. 10 (1998) 2086;
Z. Peng, Z. Bao, M.E. Galvin, Adv. Mater. 10 (1998) 680.
[13] M. Zheng, L. Ding, E.E. Gurel, P.M. Lahti, F.E. Karasz, Macromolecules 34 (2001) 4124.
[14] Z. Bao, J.A. Rogers, A. Dodabalapur, A.J. Lovinger, H.E. Katz, V.R. Raju, Z. Peng, M.E. Galvin, Opt. Mater. 12 (1999) 177;
Z. Bao, Z. Peng, M.E. Galvin, E.A. Chandross, Chem. Mater. 10 (1998) 1201.
[15] N. Miyaura, T. Yanagi, A. Suzuki, Synth. Commun. 11 (1981) 513.
[16] M.T. Bernius, M. Inbasekaran, J. O'Brien, W. Wu, Adv. Mater. 12 (2000) 1737.
[17] S. Janietz, D.D.C. Bradley, M. Grell, C. Giebeler, M. Inbasekaran, E.P. Woo, Appl. Phys. Lett. 73 (1998) 2453.
[18] M. Redecker, D.D.C. Bradley, M. Inbasekaran, E.P. Woo, Appl. Phys. Lett. 73 (1998) 1565;
M. Redecker, D.D.C. Bradley, M. Inbasekaran, W.W. Wu, E.P. Woo, Adv. Mater. 11 (1999) 241.
[19] G. Jegou, S.A. Jenekhe, Macromolecules 34 (2001) 7926.
[20] S.-J. Lee, J.R. Gallegos, J. Klein, M.D. Curtis, J. Kanicki, Proc. SPIE 4800 (2003) 123.
[21] X. Zhan, Y. Liu, X. Wu, S. Wang, D. Zhu, Macromolecules 35 (2002) 2529.
[22] J. Ding, Y. Tao, M. Day, J. Roovers, M. D'lorio, J. Opt. A Pure Appl. Opt. 4 (2002) S267;
J. Ding, M. Day, G. Robertson, J. Roovers, Macromolecules 35 (2002) 3474.
[23] F.Y. Wu, D.S. Reddy, C.F. Shu, M.S. Liu, A.K.-Y. Jen, Chem. Mater. 15 (2003) 269.
[24] D. Poplavskyy, J. Nelson, D.D.C. Bradley, Appl. Phys. Lett. 83 (2003) 707.
[25] Y. Hong, Z. He, N.S. Lennhoff, D.A. Banach, J. Kanicki, J. Electron. Mater. 33 (2004) 312.
[26] F. Bentiss, M. Lagrenée, J. Heterocyclic Chem. 36 (1999) 1029.
[27] J.K. Politis, M.D. Curtis, L. Gonzalez-Ronda, D.C. Martin, Chem. Mater. 12 (2000) 2798.
[28] J.C. de Mello, H.F. Wittmann, R.H. Friend, Adv. Mater. 9 (1997) 230.
[29] S.-J. Lee, J. Klein, J. Kanicki, Rev. Sci Instrum., in press.
[30] Y. Hong, J. Kanicki, Rev. Sci. Instrum. 74 (2003) 3572.
[31] S.-J. Lee, A. Badano, J. Kanicki, IEEE J. Sel. Top. Quantum Electron. 10 (2004) 37.

[32] N.C. Greenham, R.H. Friend, D.D.C. Bradley, Adv. Mater. 6 (1994) 491.
[33] Y. Hong, Z. Hong, M.D. Curtis, J. Kanicki, Conf. Rec. IDRC 2000 (2000) 183.
[34] Y. Hong, Z. He, S.-J. Lee, J. Kanicki, Proc. SPIE 4464 (2001) 329.
[35] S. Janietz, A. Wedel, Adv. Mater. 9 (1997) 403;
S. Janietz, D.D.C. Bradley, M. Grell, C. Giebeler, M. Inbasekaran, E.P. Woo, Appl. Phys. Lett. 73 (1998) 2543;
S. Janietz, S. Anlauf, A. Wedel, Macromol. Chem. Phys. 205 (2004) 187.
[36] G. Zeng, W.L. Yu, S.J. Chua, W. Huang, Macromolecules 35 (2002) 6907.
[37] L. Romaner, A. Pogantsch, P.S. de Freitas, U. Scherf, M. Gaal, E. Zojer, E.J.W. List, Adv. Funct. Mater. 13 (2003) 597;
E.J.W. List, R. Guentner, P.S. de Freitas, U. Scherf, Adv. Mater. 14 (2002) 374.
[38] X. Gong, P.K. Iyer, D. Moses, G.C. Bazan, A.J. Heeger, S. Xian, Adv. Mater. 13 (2003) 325.
[39] J.W.T. Walsh, Photometry, second ed., Constable and Company Ltd., London, 1953.